Author Manuscript

Author Manuscript

Author Manuscript

Author Manuscript

HHS Public Access

Author manuscript

Cancer Prev Res (Phila). Author manuscript; available in PMC 2023 January 05.

Published in final edited form as:

Cancer Prev Res (Phila). 2022 July 05; 15(7): 423–434. doi:10.1158/1940-6207.CAPR-21-0610.

Chronic exposure to waterpipe smoke elicits immunomodulatory and carcinogenic effects in the lung

Maya Hassane[1,*], **Zahraa Rahal**[2,*], **Nareg Karaoghlanian**[3], **Jiexin Zhang**[4], **Ansam Sinjab**[2], **Justin W. Wong**[5], **Wei Lu**[2], **Paul Scheet**[5], **J. Jack Lee**[4], **Maria Gabriela Raso**[2], **Luisa M Solis**[2], **Junya Fujimoto**[2], **Hassan Chami**[1,6], **Alan L. Shihadeh**[3], **Humam Kadara**[2,#]

[1]Faculty of Medicine, American University of Beirut, Beirut, Lebanon.

[2]Department of Translational Molecular Pathology, The University of Texas MD Anderson Cancer Center, Houston, Texas, USA.

[3]Faculty of Engineering, American University of Beirut, Beirut, Lebanon.

[4]Department of Biostatistics and Computational Biology, The University of Texas MD Anderson Cancer Center, Houston, Texas, USA.

[5]Department of Epidemiology, The University of Texas MD Anderson Cancer Center, Houston, Texas, USA.

[6]School of Medicine, John Hopkins University, Baltimore, Maryland, USA.

Abstract

Effects of waterpipe smoking on lung pathobiology and carcinogenesis remain sparse despite the worldwide emergence of this tobacco vector. To address this gap, we investigated the effects of chronic waterpipe smoke (WPS) exposure on lung pathobiology, host immunity, and tumorigenesis using an experimental animal model that is prone to tobacco carcinogens and an exploratory observational analysis of human waterpipe smokers and non-smokers. Mice exhibited elevated incidence of lung tumors following heavy WPS exposure (five days/week for 20 weeks) compared to littermates with light WPS (once/week for 20 weeks) or control air. Lungs of mice exposed to heavy WPS showed augmented CD8+ and CD4+ T cells counts along with elevated pro-tumor immune phenotypes including increased IL-17A in T/B cells, PD-L1 on tumor and immune cells, and the pro-inflammatory cytokine IL-1β in myeloid cells. RNA-sequencing (RNA-seq) analysis showed reduced anti-tumor immune gene signatures in animals exposed to heavy WPS relative to control air. We also performed RNA-seq analysis of airway epithelia from bronchial brushings of cancer-free waterpipe smokers and non-smokers undergoing diagnostic bronchoscopy. Transcriptomes of normal airway cells in waterpipe smokers, relative to waterpipe non-smokers, harbored gene programs that were associated with poor clinical outcomes in lung adenocarcinoma (LUAD) patients, alluding to a WPS-associated molecular injury, like that established in response to cigarette smoking. Our findings support the notion that WPS exhibits

[#]Correspondence to Humam Kadara, PhD, Department of Translational Molecular Pathology, The University of Texas MD Anderson Cancer Center, Houston, Texas, USA, Telephone: 713-745-9396, hkadara@mdanderson.org.

[*]:equally contributing co-first authors

Competing interests: HK reports funding from Johnson and Johnson outside the scope of this work. All other authors declare no potential conflicts of interest.

Author Manuscript Author Manuscript Author Manuscript Author Manuscript

carcinogenic effects and constitutes a possible risk factor for lung cancer as well as warrant future studies that can guide evidence-based policies for mitigating waterpipe smoking.

PREVENTION RELEVANCE STATEMENT—Potential carcinogenic effects of waterpipe smoking are very poorly understood despite its emergence as a socially acceptable form of smoking. Our work highlights carcinogenic effects of waterpipe smoking in the lung and, thus, accentuate the need for inclusion of individuals with exclusive waterpipe smoking in prevention and smoking cessation studies.

Keywords

Waterpipe smoke; host immune responses; lung adenocarcinoma; RNA-sequencing

INTRODUCTION

Tobacco use poses a major worldwide health concern and accounts for over 8 million deaths yearly, including 1.8 million lung cancer-related deaths (1). While cigarette smoking prevalence has declined globally in recent decades, waterpipe smoking has emerged as a significant vector for tobacco use, particularly among youth (2). The emergence of waterpipe use globally may be partly fueled by the perception that it is a safer and non-addictive alternative to cigarette smoking. In addition, attitudes towards waterpipe smoke (WPS) use are generally more accepting than for cigarette smoke (CS) (3). However, contrary to popular belief, during a typical one-hour use session, the waterpipe emits and delivers high doses of nicotine, cardiovascular and pulmonary toxicants, and carcinogens to the user (4,5) and surroundings (6). Additionally, studies have shown that the manifold “tar” and polycyclic aromatic hydrocarbons yielded by a single waterpipe smoking session exceed those generated by a single cigarette (4,5).

The extensive research on CS over the past several decades has established clear causal links between CS and lung cancer (7). It is estimated that there are more than 1.3 billion tobacco users worldwide who are at elevated risk for lung disease, including lung adenocarcinoma (LUAD), the most common lung cancer subtype (8). Similar to CS, exposure to WPS is associated with increased pulmonary inflammation and deleterious effects on both the respiratory (e.g., chronic bronchitis, emphysema) and cardiovascular systems (9,10). Furthermore, previous reports in murine models showed that WPS activates a prominent inflammatory response in the host lung (11-13). Yet, most of those studies interrogated WPS in the acute or subacute settings, and reports on the effects of chronic waterpipe exposure, remain limited (12-15). Importantly, effects of chronic exposure to WPS on lung carcinogenesis are unknown.

To begin to address this gap, in this study we sought to investigate the effects of chronic WPS exposure on lung pathobiology and host immunity in an animal model and in human participants. We compared lung immune responses and tumorigenesis in mice exposed to a one-hour WPS session for 20 weeks in a whole-body exposure system, once a week (light WPS) or five times a week (heavy WPS), relative to control mice exposed to ambient air. We also compared the transcriptomes of normal-appearing airway cells from bronchoscopy samples in human waterpipe smokers and non-smokers.

Author Manuscript Author Manuscript Author Manuscript Author Manuscript

MATERIALS AND METHODS

Smoke exposure system

A whole-body waterpipe smoke exposure system was designed and built for this study at the American University of Beirut (AUB) Aerosol Research Lab (Figure 1). Smoke was drawn intermittently by a positive pressure smoking machine and discharged into a transparent polycarbonate chamber (38x25x25 cm) containing the animals. During each one-hour exposure session, each puff was entirely discharged into the chamber. Ambient air was continuously pumped into the chamber at a flow rate of 0.5 liters per minute (LPM), resulting in approximately 1.25 air changes per hour, not including the intermittent smoke flow. A carbon monoxide (CO) analyzer (Bacharach Monoxor III) drawing a sample flow of 0.3 LPM was used to monitor CO levels in the chamber, and a 3 cm diameter fan was suspended from the top to ensure uniform aerosol concentrations throughout the chamber. A glass fiber filter (Gelman Type A/E) was placed upstream of the CO monitor to allow gravimetric determination of the mean total particulate matter concentration during each exposure session. For the control group, the smoking machine was switched off and animals were exposed to ambient air only.

Smoke generation protocol

A waterpipe (53 cm overall height) fitted with a leather hose with an infiltration rate of below 2 LPM, as previously measured per Saleh and Shihadeh (16), was used in this study. Prior to each session, the waterpipe was loaded with 10 g of “two apples” flavor, “Nakhla” brand tobacco. A single quick light charcoal disk (“Three Kings” brand) was placed on top of the tobacco mix prior to smoking, and an additional half-disk was added at the 105^{th} puff. The smoking machine was programmed to draw 171 puffs of 2.6 s duration and 17 s interpuff interval, at a mean flow rate of 12 LPM, as per the Beirut Protocol (17). Further details about the waterpipe preparation and the charcoal application were previously reported (18).

Animal housing and WPS exposure experiments

Animal studies were conducted under institutional animal care and use committee (IACUC)–approved protocols. *Gprc5a*$^{-/-}$;*Lcn2*$^{-/-}$ mice were generated as previously described (8), and 8-9 weeks old mice (males and females) were divided into groups of up to five mice (per exposure group and time point) and were exposed (full-body) during a one-hour session to control air or to light or heavy WPS (1 time or 5 times per week, respectively) for 20 weeks. Different groups of mice were humanely euthanized immediately at the end of exposure for immune analyses or after 20 weeks following end of exposure for sequencing and histopathological assessment of lungs.

Histopathological analysis of mouse lung lesions

Lungs were inflated with formalin, excised, and macroscopically examined for surface lesions before being processed for histopathological assessment. Formalin-fixed lungs were embedded in paraffin, and four deep sections (four micron each) were acquired form each fixed lung, stained with hematoxylin and eosin (H&E), digitally scanned using the Aperio

Author Manuscript Author Manuscript Author Manuscript Author Manuscript

ScanScope Turbo slide scanner (Leica Microsystems Inc.) at 200X magnification, and visualized by ImageScope software (Leica Microsystems, Inc.). Images were analyzed by a well-experienced pathologist who was blinded to groups to identify the tumors.

Flow cytometry

Lungs were perfused with PBS containing 2% fetal calf serum (FCS), excised and finely minced, followed by enzymatic digestion for 30 min at 37°C in PBS containing 150U/ml collagenase type IV and 20 U/ml DNase type I. Lung homogenates were suspended in a 20% Percoll gradient and centrifuged. Pellets were then washed, and red blood cells lysed. Cells were incubated in RPMI 10% FCS containing Golgi Plug/Golgi Stop for 2 hours at 37°C. Cells were then stained for 30 minutes with fluorescence-conjugated antibodies (Biolegend or Becton Dickinson) diluted in PBS 2% FCS: anti-CD45 (AF700-conjugated), anti-Ly6G (FITC-conjugated), anti-CD11b (PerCpCy5.5-conjugated), anti-SiglecF (APCCy7-conjugated), anti-CD11c (FITC-conjugated), anti-MHCII (PerCpCy5.5-conjugated), anti-F4/80 (PeCy7-conjugated), anti-CD4 (FITC-conjugated), anti-CD8 (APCCy7-conjugated), anti-B220 (PerCpCy5.5-conjugated) and anti-PD-L1 (PeCy7-conjugated). Cells were washed and fixed, permeabilized, and stained with PE-conjugated antibodies against pro-IL-1β (Thermofisher) or IL-17A (Biolegend) and analyzed on a BD Aria cell sorter. Flow cytometry analyses were performed using the Diva software.

Collection of human bronchial epithelial brushings

Participants were identified prior to undergoing routine bronchoscopy at the Department of Internal Medicine at American University of Beirut Medical Center (AUBMC) in Beirut Lebanon. Eligible patients were selected from a cohort of prospectively acquired bronchial brushings from consented patients with or without lung lesions (suspect or already cytopathologically confirmed to be malignant) who are undergoing routine diagnostic bronchoscopy at the Department of Internal Medicine at AUBMC under a protocol approved by the institutional review board. Written informed consents were obtained from all participants and the studies were conducted in accordance with the ethical guidelines of the Declaration of Helsinki. Inclusion criteria included: 1) non-smokers, former or current smokers (cigarette, cigar, waterpipe) who are scheduled to undergo bronchoscopy; 2) age ≥ 18 years old; 3) no intercurrent illness such as another active malignancy, and active infectious bronchitis at time of bronchoscopy. Exclusion criteria included: 1) pregnant females; 2) contraindications to fiberoptic bronchoscopy including hemodynamic instability, decompensated heart failure, recent myocardial infarction within 6 weeks, uncontrolled arrythmias, high risk for respiratory failure, uncontrolled asthma, severe obstructive airway disease (as determined by spirometry); 3) contraindications to brushing/biopsy: patients at risk of bleeding (e.g. with known bleeding disorders and abnormal coagulation platelets count <50,000; INR>1.5,PTT>50 seconds); 4) suspected active pulmonary tuberculosis; 5) known human immunodeficiency virus HIV; 6) patients who are unable to consent. Bronchoscopy and collection of airway epithelia from bronchial brushings were done as previously described (19).

Participants were surveyed for demographic characteristics, bronchoscopy indication, presence of underlying lung disease, malignancy diagnosis (type and date of diagnosis

Author Manuscript Author Manuscript Author Manuscript Author Manuscript

status), occupational/environmental exposures and smoking habits (type, duration and intensity) using investigator administered questionnaires. Individuals who have never smoked a waterpipe or have smoked less than 100 waterpipes in their lifetime were categorized as waterpipe non-smokers. Waterpipe smokers included those who smoked at least 100 waterpipes during their life and are currently smoking and those who quit smoking less than 12 months before enrollment. Individuals who smoked at least 100 waterpipes during their life and quit smoking more than 12 months before enrollment were considered former waterpipe smokers. We also studied five lung cancer-free individuals who never smoked waterpipe and were categorized as waterpipe non-smokers and four lung cancer-free individuals who smoked at least 100 waterpipes in their lifetime, including during the 12-month period prior to enrollment, categorized as waterpipe smokers. One waterpipe non-smoker was a former light cigarette smoker for two years and quit 31 years prior to enrollment. Age, sex and smoking history of those nine participants are summarized in Supplementary Table 1.

Enzyme-linked immunosorbent assay (ELISA)

Bronchoalveolar lavage fluid (BALF) was collected from mice exposed to control air, light, and heavy WPS. IL-17A (eBiosciences) levels in the supernatants were measured by ELISA as described previously.

Total RNA isolation from mouse lung tissues and human airway epithelia

Total RNA was isolated from homogenized tissues (mouse lungs and human bronchial airway epithelia) using Qiagen RNeasy mini kit (Qiagen) according to manufacturer's recommendations. Qubit 4 Fluorometer (Thermo Fisher Scientific, Waltham, MA) was used for measurement of RNA yield, and RNA quality was assessed by NanoDrop 1000 (Thermo Fisher Scientific) as well as the Agilent RNA 6000 Pico Kit (Agilent, Santa Clara, CA) for computation of RNA integrity numbers.

RNA-sequencing and analysis

At least 10 ng of input RNA were used for generation of barcoded cDNA transcriptome libraries using the SMARTer seq V3, Takara Bio Kit (Takara, Mountain View, CA) adhering to the manufacturer's protocol. Libraries were then sequenced using NovaSeq 6000 platform from Illumina at a target coverage of 40 million reads per sample. All raw data are uploaded to the gene expression omnibus (GEO). Alignment and mapping was performed using STAR (20). Genes with no coverage in >50% of samples were filtered. DESEQ2 (21) was applied for identification of differentially expressed genes (DEGs) using p-values that were adjusted using the Benjamini-Hochberg methods. DEGs were analyzed by pathways analysis or topologically organized into gene networks using Ingenuity Pathways Analysis (8).

Pathways and gene network analysis as well as in silico assessment of gene signatures

Following RNA-seq of *Gprc5a*$^{-/-}$;*Lcn2*$^{-/-}$ mouse lung tissues at 20 weeks following control air or heavy WPS exposure, differentially expressed genes were organized into pathways and topological gene-gene interaction networks using Ingenuity Pathways Analysis as described previously (22). Immune signatures were curated from the previous reports: Cytotoxic

Author Manuscript Author Manuscript Author Manuscript Author Manuscript

T lymphocyte derived by Jiang and colleagues (CTL; *Cd8a, Cd8b, Gzma, Gzmb, Prf1*; (23)); T cell expanded signature by Ayers and colleagues (Expanded signature; *Cd3d, Ido1, Ciita, Cd3e, Ccl5, Gzmk, Cd2, Hla-Dra, Cxcl13, Il2rg, Nkg7, Hla-E, Cxcr6, Lag3, Tagap, Cxcl10, Stat1, Gzmb*; (24)); and T effector signature by McDermott and colleagues (*Cd8A, Eomes, Prf1, Ifng, Cd274;* (25)). We also interrogated the expression of a gene signature that is prognostic in lung adenocarcinoma (LUAD) and previously published by Wang and colleagues (ARNTL2, *PLA2G4F, CYP17A1, LOXL2, HMMR, NKX2-5, GJB2, DSG3, SIX1, MC4R, TRPA1, RAET1L, KLF4, HSF2BP, GRIP1, PTPRN, MAPK4, PLOD2*; (26)) in our RNA-seq cohort of airways of waterpipe smokers and non-smokers. For each of the signatures, the average of regularized log transformed values of the signature's gene members were computed and statistically compared between samples using the Wilcoxon rank sum test. Survival analysis was performed in treatment-naïve LUAD patients (n = 508) from the publicly available TCGA cohort (27), and from the PROSPECT dataset (Profiling of Resistance Patterns and Oncogenic Signaling Pathways in Evaluation of Cancers of the Thorax, n = 152; (28)). Patients were dichotomized into upper and lower quartiles based on median values of the prognosis signature. Statistical differences in survival between different groups were evaluated in R using the log-rank test and the Kaplan–Meier method for estimation of survival probability.

Statistical analysis

GraphPad Prism software and the R statistical language and environment (r-project.org) were used for statistical analyses. Pearson correlation coefficients were used to statistically examine correlations between continuous variables. To establish statistical significance of differences in specific contrasts between two groups, we used Student's t-test or Wilcoxon rank-sum test. To evaluate statistical differences among three or more groups, we used ANOVA or Kruskal-Wallis tests. Statistical significance was achieved with *p*-values less than 0.05.

DATA AVAILABILITY

Raw RNA-seq data of lungs of *Gprc5a*$^{-/-}$;*Lcn2*$^{-/-}$ mice at 20 weeks following end of exposure to control air or heavy WPS exposure were deposited into gene expression omnibus (GEO) as GSE197994. Raw RNA-seq data of airway epithelia from bronchial brushings of patients undergoing bronchoscopy were deposited into GEO as GSE197653.

RESULTS

Effects of chronic waterpipe exposure on lungs of mice

To begin to understand the impact of chronic WPS exposure on lung cancer development, a whole body WPS exposure system was exclusively designed for this study. We studied *Gprc5a*$^{-/-}$;*Lcn2*$^{-/-}$ mice, which we previously showed to be highly susceptible to nicotine-specific carcinogen-mediated lung cancer development (8), despite being of the C57/BL6 strain that is resistant to tobacco carcinogens (29). Mice were exposed to whole-body WPS or control ambient air. The smoking machine was programmed per the Beirut protocol (17). Mice were chronically exposed to 1 (light WPS) or 5 (heavy WPS) of these smoking sessions per week, and for 20 weeks (Figure 1). At 20 weeks following end of exposure,

Author Manuscript Author Manuscript Author Manuscript Author Manuscript

histopathological analysis revealed lung tumor formation in animals exposed to WPS but not in animals exposed to control air (Figure 2A). Fraction of mice with lung tumor development was higher in mice with heavy (five days a week) relative to light (once a week) WPS exposure or control air-exposed animals ($P < 0.0001$ of the Chi-squared test; Figure 2B). The higher incidence in the heavy WPS-exposed group was complemented by a higher average total tumor volume compared to light WPS-exposed animals (Supplementary Table 2). Furthermore, we found Ki-67 nuclear staining in cells within lung tumors suggesting a proliferative feature of these lesions (Figure 2C). These findings suggest that WPS exposure promotes lung tumor formation. They also demonstrate that lung tumor formation is increased with more frequent WPS exposure.

Exposure to WPS modulates host lung immune responses

We were prompted to examine changes in the lung immune microenvironment by WPS exposure and prior to LUAD formation (Figure 1). Flow cytometry analysis of mouse lung mononuclear cells revealed a significant decrease in dendritic cells in mice exposed to heavy WPS compared to control air ($P < 0.05$; Figure 3A). In contrast to ambient air-exposed mice, littermates with WPS exposure showed significantly increased CD4+ T cell counts ($P < 0.05$; Figure 3A). These effects were more pronounced in mice with heavy WPS exposure (Figure 3A). Mice exposed to light WPS also showed significantly elevated CD8+ T cell counts ($P < 0.05$; Figure 3A). We noted no significant differences in neutrophil, macrophage, alveolar macrophage and B cell counts across the three different exposure groups (Figure 3A). We then probed the expression of pro-inflammatory immune markers. We found that IL-17A protein expression in CD4+ and CD8+ T as well as B cells was significantly enriched in lungs of mice exposed to WPS compared to control air counterparts ($P < 0.05$) (Figure 3B). We concordantly found significantly increased levels of IL-17A protein in BALF of WPS-exposed mice compared to control air-exposed littermates ($P < 0.05$ for the heavy WPS group; Figure 3C). We noted trends for increased IL-17A protein in lung and BALF of heavy relative to light WPS-exposed mice (Figures 3B and 3C). We also found that levels of the pro-inflammatory cytokine pro-IL-1β in neutrophils ($P < 0.05$) and dendritic cells ($P < 0.01$) were significantly increased following chronic exposure to light or heavy WPS (Supplementary Figure 1A). Intriguingly, expression of the major pro-tumor immune checkpoint programmed cell death marker ligand (PD-L1) was significantly increased in neutrophils and macrophages following light or heavy WPS exposure ($P < 0.05$; Supplementary Figure 1B). Furthermore, we also noted PD-L1 staining on epithelial cells in tumors (Figure 2C).

We then performed RNA-sequencing (RNA-seq) analysis of lungs of *Gprc5a*$^{-/-}$;*Lcn2*$^{-/-}$ mice 20 weeks following exposure to control air or heavy WPS (Figure 1). We identified 4,262 gene transcripts that were differentially and significantly modulated** (based on an adjusted *P*-value threshold of 0.01 and a fold-change of at least 1.5) between heavy WPS and control air exposed mice (Figure 4A). Lungs of mice heavily exposed to WPS exhibited overall markedly increased activation of oxidative phosphorylation genes ($P < 0.05$; Figure 4B). Conversely, we noted significant inhibition of phagosome formation in heavy WPS-exposed animals ($P < 0.05$; Figure 4B) which was consistent with our observation of reduced counts of dendritic cells by flow cytometry following WPS (Figure

Author Manuscript Author Manuscript Author Manuscript Author Manuscript

3A). We then analyzed immune gene sets curated from the literature (25,30,31). We found significantly attenuated cytotoxic T-lymphocytes ($P < 0.05$), expanded immune ($P < 0.05$), and T-effector ($P < 0.001$) signatures following heavy WPS exposure compared to control air (Figure 4C), suggesting that while T cell counts may have been increased in WPS-exposed animals (Figure 3A), they may be dysfunctional or exhausted (32). Intriguingly, we found, among genes that were differentially expressed in mice heavily exposed to WPS, increased expression ($P < 0.001$) of *Tmprss4*, *Cd55*, and *Ace2* which are known to be important for SAR-COV-2 viral entry into host airway cells and contraction of COVID-19 (Figure 4D). Our data collectively suggest that WPS exposure suppresses key anti-tumor immune functions and modulates the host lung immune contexture by skewing it to a pro-tumorigenic inflammatory state.

Airways of waterpipe smokers exhibit gene signatures prognostic of lung adenocarcinoma

Previous work from our group and others revealed that CS-exposed normal-appearing airways in LUAD patients carry alterations that are characteristic of the adjacent LUADs (33), suggestive of a field of injury that is pertinent to carcinogenesis. Also considering our murine findings on lung tumor development and immune modulation following WPS exposure, we were thus prompted to interrogate normal-appearing human airways of cancer-free waterpipe smokers relative to those who did not smoke waterpipe. To this end, we studied bronchial brushings from patients undergoing diagnostic bronchoscopy including 4 lung cancer-free smokers (smoked at least 100 waterpipes in their lifetimes) and 5 lung cancer-free non-smokers (never smoked a waterpipe or smoked < 100 waterpipes). The non-smoker group comprised CS non-smokers except for one case who was a light former CS smoker (< 2 lifetime pack-years who quit 20 years ago) (Supplementary Table 1). We analyzed gene expression of airway epithelia from the bronchial brushings of those subjects by RNA-seq (Figure 5A). We identified 168 gene transcripts (Supplementary Table 3) that were significantly modulated (based on an adjusted *P*-value threshold of 0.05) between waterpipe smokers and non-smokers (Figure 5B). Normal bronchial brushings of waterpipe smokers **showed increased activation of the NRF-2 mediated oxidative stress response pathway (Figure 5C), consistent with our findings in mice heavily exposed to WPS (Figure 4B).

We also interrogated the expression of a previously reported gene signature that is prognostic in lung adenocarcinoma (LUAD) (*ARNTL2*, *PLA2G4F*, *CYP17A1*, *LOXL2*, *HMMR*, *NKX2*-5, *GJB2*, *DSG3*, *SIX1*, *MC4R*, *TRPA1*, *RAET1L*, *KLF4*, *HSF2BP*, *GRIP1*, *PTPRN*, *MAPK4*, *PLOD2*) in our RNA-seq cohort of airways of waterpipe smokers and non-smokers (26). We found that this gene set was indeed associated with reduced overall survival when we analyzed LUADs from The Cancer Genome Atlas (TCGA; $P = 0.0007$; Figure 5D, left panel) and our previously reported PROSPECT cohort (28) ($P = 0.03$, PFI; Figure 5D, middle panel) datasets. Notably, we found that these genes were enriched in airways of waterpipe smokers relative to non-smokers ($P < 0.05$; Figure 5D, right panel). Our analyses underscore transcriptomic alterations in normal-appearing airways of cancer-free waterpipe smokers that are indicative of LUAD pathogenesis. Intriguingly, and similar to our findings in mice exposed to heavy WPS, we found increased expression ($P < 0.01$) of *TMPRSS4* in airway epithelia of waterpipe smokers. We also noted increased levels of

Author Manuscript Author Manuscript Author Manuscript Author Manuscript

CD55 and *ACE2* in airways of waterpipe smokers albeit not reaching statistical significance (Supplementary Figure 2).

DISCUSSION

Research efforts focused on the effects of waterpipe smoking on the lung remain sparse despite its worldwide emergence as a socially acceptable form of smoking, particularly among the youth (2). There is a pressing need to better understand the effects of this form of smoking on lung pathophysiology, particularly lung cancer. Here, we interrogated the effects of WPS exposure on mice known to be susceptible to carcinogen mediated LUAD development. We found that WPS exposure was associated with increased lung tumor formation in mice** and was more pronounced following a heavier WPS exposure regimen. Lungs of WPS-exposed mice also exhibited a modulated host lung immune microenvironment that favored a pro-tumorigenic inflammatory state. We further assessed the effects of WPS exposure on normal-appearing airways of cancer-free waterpipe smokers. We found that transcriptomes of normal airway cells from waterpipe smokers, relative to non-smokers, exhibited pronounced immunomodulation as well as genes that were associated with poor survival among LUAD patients -- thereby supporting the supposition that waterpipe smokers might be at a heightened risk of developing lung cancer.

We found that mice subjected to WPS were more likely to develop lung tumors. Further validation is needed to establish an empirical link between WPS and lung cancer development, in additional animal models. While we found significantly increased CD4 and CD8 T cells counts in lungs of WPS-exposed mice, our RNA-seq analysis showed that signatures of cytotoxic or expanded immune response were, conversely, decreased in animals exposed to heavy WPS relative to control air. In spite that these observations may at first appear contrary to each other, they perhaps suggest that T cell populations in WPS-exposed animals may be dysfunctional or exhausted. Our findings and supposition are in line with previous reports showing that cigarette smoking exerts immunosuppressive effects on the tumor immune microenvironment by hampering cytotoxic T cells and causing a predominant state of T cell anergy (32). Levels of the pro-inflammatory cytokines IL-17, and pro-IL-1β, were also increased post-WPS exposure. IL-17-mediated inflammatory responses have been shown to be key in the progression of cancer, particularly lung tumors (34). Our findings resonate with trends observed in our murine model which had increased production of IL-17A by CD4+ and CD8+ positive T cells during tumor development upon exposure to chemical-induced carcinogenesis (8). Moreover, evidence suggests a pivotal role for IL-1β in inflammation and possibly in lung cancer pathogenesis (35). Indeed, the IL-1β antibody canakinumab significantly reduced lung cancer incidence and mortality in a high-risk population (36). Our findings are also in line with previously reported effects of tobacco and waterpipe exposure, such as the activation of host defense inflammatory mechanisms (11-13,15) with pro-tumor effects (37). Another worthy observation was the increased expression of the major immune checkpoint PD-L1 protein in neutrophils and macrophages following WPS exposure. PD-L1 plays important roles in immune suppression and evasion, and anti-PD-L1 antibodies are approved for immunotherapy of lung cancer (38). Indeed, a study investigating the effects of chronic waterpipe exposure described immune suppressive effects that are comparable to our observations (39). It is thus plausible

Author Manuscript Author Manuscript Author Manuscript Author Manuscript

that WPS exposure leads to early immune suppression and evasion which promote lung carcinogenesis.

When analyzing the transcriptome of airways of cancer-free patients exposed to WPS, we found significant activation of genes related to the NRF-2 mediated oxidative stress response, in line with a previous report probing epigenetic changes in the small airway epithelium of waterpipe smokers (14). This was also concordant with the activation of oxidative phosphorylation pathways in lungs of mice heavily exposed to WPS. Indeed, smoking has been shown to induce the production of reactive oxygen species by oxidative phosphorylation (40). Furthermore, our findings allude to a possible molecular airway *field of injury* similar to that established, at the transcriptomic level, in response to CS (33,41,42). Our data also suggest that transcriptomes of normal airway cells in waterpipe smokers, relative to waterpipe non-smokers, harbor gene programs that are associated with poor clinical outcome in LUAD patients, also suggestive of a WPS-associated molecular *injury* that may inform of LUAD pathogenesis. Thus, we provide evidence, albeit preliminary, that WPS may elicit an airway field of injury that, based on its molecular (e.g., gene signatures) and immune (e.g., pro-inflammatory milieu) features, favors lung carcinogenesis. It is noteworthy to point that in mice heavily exposed to WPS, we found increased expression of *Tmprss4*, *Cd55*, and *Ace2,* key mediators for the entry of SAR-COV-2 virus implicated in COVID-19 disease (43). Upregulation of pulmonary *ACE2* in smokers has been previously reported and suggested to increase susceptibility for SARS-CoV-2 infection (44). For instance, cigarette smoking is known to induce goblet cells metaplasia (main source of ACE2 in the lungs) by epigenetic alterations (45), partly explaining the increased expression of *ACE2* in smokers. Therefore, it is not unlikely that waterpipe smokers might also be at higher risk of infection by mechanisms that are yet to be discovered. This assumption requires further validation to cognize its relevance, especially that the effect of smoking on the development of COVID-19 pneumonia remains controversial (46).

Our study incurred several limitations. Using our mouse model, we show increased lung tumor development following a one-hour waterpipe session, loaded with a particular type of tobacco and charcoal. Those findings ought not to be underappreciated but should be interpreted cautiously as further studies are warranted to replicate our findings using different types of waterpipe tobacco and charcoal, as well as in other mouse models. Indeed, comparison of WPS exposure to positive controls with **well-known **carcinogenic effects in the lung (such as tobacco carcinogen as chemical or inhaled cigarette smoke) is also warranted to better corroborate our findings. While we show increased tumor development in mice exposed to waterpipe using our whole-body exposure system, our findings will need to be validated using systems that better simulate human waterpipe smoking. For instance, exposure systems that can ensure enhanced inhalational efficacy while minimizing particulate deposition on animal fur are desired to draw solid conclusions from murine models. Furthermore, behavioral studies on waterpipe consumption show that a single waterpipe session can last longer than an hour (47), making our employed smoking protocol ungeneralizable to all WPS regimens. It is thus, plausible to surmise that different smoking protocols using distinct or combinations of different waterpipe tobacco and charcoal types can lead to various other molecular (e.g., gene signatures) and immune (e.g., pro-inflammatory milieu). While we provide support for the hypothesis that WPS

Author Manuscript Author Manuscript Author Manuscript Author Manuscript

exposure increases lung cancer risk in humans, based on lung tumor-associated gene profiles in exposed epithelia, this supposition warrants further validation in a larger cohort of non-smokers and exclusive waterpipe smokers. Additionally, and due to the worldwide spread of waterpipe smoking, more efforts are needed to interrogate WPS cohorts that extend beyond Middle Eastern countries which have constituted the major geographical focus in published WPS reports thus far (9-12,15,48,49). Furthermore, epidemiological studies suggest that many smokers are exposed to both CS and WPS throughout their lifetime (48,49). This "concoction" of exposures may lead to an increased susceptibility to various lung diseases, such as lung cancer, compared to exclusive waterpipe or cigarette smoking. Therefore, future studies are warranted to better elucidate the consequences of being exposed to a combination of both waterpipe and CS.

In conclusion, we show that WPS exposure leads to lung tumor formation in mice and elicits molecular and immune features that are informative of the pathogenesis of lung cancer, and, thus, risk for the disease. Additional studies are needed to fully assess procarcinogenic effects of WPS, and to demand a resurgence of attention to this topic in terms of evidence-based science policy enactment, which includes but is not limited to regulation of WPS products' consumer age and availability, packaging warning labels, and the use of WPS in public spaces (50).

Supplementary Material

Refer to Web version on PubMed Central for supplementary material.

Grant support:

Funded in part by the National Cancer Institute (NCI) grant R01CA205608 (to H. Kadara) and an MPP grant from the American University of Beirut (to H. Chami).

REFERENCES

1. Thandra KC, Barsouk A, Saginala K, Aluru JS, Barsouk A. Epidemiology of lung cancer. Contemp Oncol (Pozn) 2021;25(1):45–52 doi 10.5114/wo.2021.103829. [PubMed: 33911981]
2. Rahal Z, El Nemr S, Sinjab A, Chami H, Tfayli A, Kadara H. Smoking and Lung Cancer: A Geo-Regional Perspective. Front Oncol 2017;7:194 doi 10.3389/fonc.2017.00194. [PubMed: 28920053]
3. Aljarrah K, Ababneh ZQ, Al-Delaimy WK. Perceptions of hookah smoking harmfulness: predictors and characteristics among current hookah users. Tobacco induced diseases 2009;5(1):16 doi 10.1186/1617-9625-5-16. [PubMed: 20021672]
4. Shihadeh A, Schubert J, Klaiany J, El Sabban M, Luch A, Saliba NA. Toxicant content, physical properties and biological activity of waterpipe tobacco smoke and its tobacco-free alternatives. Tobacco Control 2015;24(Suppl 1):i22–i30 doi 10.1136/tobaccocontrol-2014-051907. [PubMed: 25666550]
5. Sepetdjian E, Shihadeh A, Saliba NA. Measurement of 16 polycyclic aromatic hydrocarbons in narghile waterpipe tobacco smoke. Food and Chemical Toxicology 2008;46(5):1582–90 doi 10.1016/j.fct.2007.12.028. [PubMed: 18308445]
6. Moon KA, Rule AM, Magid HS, Ferguson JM, Susan J, Sun Z, et al. Biomarkers of Secondhand Smoke Exposure in Waterpipe Tobacco Venue Employees in Istanbul, Moscow, and Cairo. Nicotine Tob Res 2018;20(4):482–91 doi 10.1093/ntr/ntx125. [PubMed: 28582531]

Author Manuscript Author Manuscript Author Manuscript Author Manuscript

7. Proctor RN. The history of the discovery of the cigarette–lung cancer link: evidentiary traditions, corporate denial, global toll. Tobacco Control 2012;21(2):87 doi 10.1136/tobaccocontrol-2011-050338. [PubMed: 22345227]
8. Treekitkarnmongkol W, Hassane M, Sinjab A, Chang K, Hara K, Rahal Z, et al. Augmented Lipocalin-2 Is Associated with Chronic Obstructive Pulmonary Disease and Counteracts Lung Adenocarcinoma Development. American Journal of Respiratory and Critical Care Medicine 2021;203(1):90–101 doi 10.1164/rccm.202004-1079OC. [PubMed: 32730093]
9. Ali M, Jawad M. Health Effects of Waterpipe Tobacco Use: Getting the Public Health Message Just Right. Tob Use Insights 2017;10:1179173X17696055–1179173X doi 10.1177/1179173X17696055.
10. Darawshy F, Abu Rmeileh A, Kuint R, Berkman N. Waterpipe smoking: a review of pulmonary and health effects. European Respiratory Review 2021;30(160):200374 doi 10.1183/16000617.0374-2020. [PubMed: 33980668]
11. Khabour OF, Alzoubi KH, Al-Sawalha N, Ahmad MB, Shihadeh A, Eissenberg T. The effect of chronic exposure to waterpipe tobacco smoke on airway inflammation in mice. Life Sci 2018;200:110–4 doi 10.1016/j.lfs.2018.03.034. [PubMed: 29555589]
12. Al-Sawalha NA, Al-Bo'ul HF, Alzoubi KH, Khabour OF, Thanawala VJ. Effect of prenatal waterpipe tobacco smoke on airway inflammation in murine model of asthma of adult offspring mice. Inhalation Toxicology 2017;29(8):366–73 doi 10.1080/08958378.2017.1385113. [PubMed: 29039230]
13. Khan NA, Sundar IK, Rahman I. Strain- and sex-dependent pulmonary toxicity of waterpipe smoke in mouse. Physiol Rep 2018;6(3) doi 10.14814/phy2.13579.
14. Walters MS, Salit J, Ju JH, Staudt MR, Kaner RJ, Rogalski AM, et al. Waterpipe smoking induces epigenetic changes in the small airway epithelium. PLoS ONE 2017;12(3):e0171112 doi 10.1371/journal.pone.0171112. [PubMed: 28273093]
15. Abi-Gerges A, Dagher-Hamalian C, Abou-Khalil P, Chahine JB, Hachem P, Khalil C. Evaluation of waterpipe smoke toxicity in C57BL/6 mice model. Pulm Pharmacol Ther 2020;63:101940 doi 10.1016/j.pupt.2020.101940. [PubMed: 32889155]
16. Saleh R, Shihadeh A. Elevated toxicant yields with narghile waterpipes smoked using a plastic hose. Food Chem Toxicol 2008;46(5):1461–6 doi 10.1016/j.fct.2007.12.007. [PubMed: 18207299]
17. Katurji M, Daher N, Sheheitli H, Saleh R, Shihadeh A. Direct measurement of toxicants inhaled by water pipe users in the natural environment using a real-time in situ sampling technique. Inhal Toxicol 2010;22(13):1101–9 doi 10.3109/08958378.2010.524265. [PubMed: 21062108]
18. Shihadeh A, Saleh R. Polycyclic aromatic hydrocarbons, carbon monoxide, "tar", and nicotine in the mainstream smoke aerosol of the narghile water pipe. Food Chem Toxicol 2005;43(5):655–61 doi 10.1016/j.fct.2004.12.013. [PubMed: 15778004]
19. Kadara H, Sivakumar S, Jakubek Y, Lucas FAS, Lang W, McDowell T, et al. Driver Mutations in Normal Airway Epithelium Elucidate Spatiotemporal Resolution of Lung Cancer. American journal of respiratory and critical care medicine 2019;200(6):742–50 doi 10.1164/rccm.201806-1178OC. [PubMed: 30896962]
20. Dobin A, Davis CA, Schlesinger F, Drenkow J, Zaleski C, Jha S, et al. STAR: ultrafast universal RNA-seq aligner. Bioinformatics 2012;29(1):15–21 doi 10.1093/bioinformatics/bts635. [PubMed: 23104886]
21. Love MI, Huber W, Anders S. Moderated estimation of fold change and dispersion for RNA-seq data with DESeq2. Genome biology 2014;15(12):550 doi 10.1186/s13059-014-0550-8. [PubMed: 25516281]
22. Caetano MS, Hassane M, Van HT, Bugarin E, Cumpian AM, McDowell CL, et al. Sex specific function of epithelial STAT3 signaling in pathogenesis of K-ras mutant lung cancer. Nature communications 2018;9(1):4589 doi 10.1038/s41467-018-07042-y.
23. Jiang P, Gu S, Pan D, Fu J, Sahu A, Hu X, et al. Signatures of T cell dysfunction and exclusion predict cancer immunotherapy response. Nature medicine 2018;24(10):1550–8 doi 10.1038/s41591-018-0136-1.
24. Ayers M, Lunceford J, Nebozhyn M, Murphy E, Loboda A, Kaufman DR, et al. IFN-gamma-related mRNA profile predicts clinical response to PD-1 blockade. The Journal of clinical investigation 2017;127(8):2930–40 doi 10.1172/jci91190. [PubMed: 28650338]

Author Manuscript Author Manuscript Author Manuscript Author Manuscript

25. McDermott DF, Huseni MA, Atkins MB, Motzer RJ, Rini BI, Escudier B, et al. Clinical activity and molecular correlates of response to atezolizumab alone or in combination with bevacizumab versus sunitinib in renal cell carcinoma. Nature medicine 2018;24(6):749–57 doi 10.1038/s41591-018-0053-3.

26. Wang L, Luo X, Cheng C, Amos CI, Cai G, Xiao F. A gene expression-based immune signature for lung adenocarcinoma prognosis. Cancer immunology, immunotherapy : CII 2020;69(9):1881–90 doi 10.1007/s00262-020-02595-8. [PubMed: 32372138]

27. Comprehensive molecular profiling of lung adenocarcinoma. Nature 2014;511(7511):543–50 doi 10.1038/nature13385. [PubMed: 25079552]

28. Skoulidis F, Byers LA, Diao L, Papadimitrakopoulou VA, Tong P, Izzo J, et al. Co-occurring genomic alterations define major subsets of KRAS-mutant lung adenocarcinoma with distinct biology, immune profiles, and therapeutic vulnerabilities. Cancer discovery 2015;5(8):860–77 doi 10.1158/2159-8290.Cd-14-1236. [PubMed: 26069186]

29. Hollander MC, Balogh AR, Liwanag J, Han W, Linnoila RI, Anver MR, et al. Strain-specific spontaneous and NNK-mediated tumorigenesis in Pten+/− mice. Neoplasia (New York, NY) 2008;10(8):866–72 doi 10.1593/neo.08406.

30. Jiang P, Gu S, Pan D, Fu J, Sahu A, Hu X, et al. Signatures of T cell dysfunction and exclusion predict cancer immunotherapy response. Nature medicine 2018;24(10):1550–8 doi 10.1038/s41591-018-0136-1.

31. Ayers M, Lunceford J, Nebozhyn M, Murphy E, Loboda A, Kaufman DR, et al. IFN-γ-related mRNA profile predicts clinical response to PD-1 blockade. The Journal of clinical investigation 2017;127(8):2930–40 doi 10.1172/jci91190. [PubMed: 28650338]

32. de la Iglesia JV, Slebos RJC, Martin-Gomez L, Wang X, Teer JK, Tan AC, et al. Effects of Tobacco Smoking on the Tumor Immune Microenvironment in Head and Neck Squamous Cell Carcinoma. Clinical Cancer Research 2020;26(6):1474 doi 10.1158/1078-0432.CCR-19-1769. [PubMed: 31848186]

33. Kadara H, Fujimoto J, Yoo SY, Maki Y, Gower AC, Kabbout M, et al. Transcriptomic architecture of the adjacent airway field cancerization in non-small cell lung cancer. Journal of the National Cancer Institute 2014;106(3):dju004 doi 10.1093/jnci/dju004. [PubMed: 24563515]

34. Chang SH, Mirabolfathinejad SG, Katta H, Cumpian AM, Gong L, Caetano MS, et al. T helper 17 cells play a critical pathogenic role in lung cancer. Proc Natl Acad Sci U S A 2014;111(15):5664–9 doi 10.1073/pnas.1319051111. [PubMed: 24706787]

35. Garon EB, Chih-Hsin Yang J, Dubinett SM. The Role of Interleukin 1β in the Pathogenesis of Lung Cancer. JTO Clin Res Rep 2020;1(1):100001 doi 10.1016/j.jtocrr.2020.100001. [PubMed: 34589908]

36. Ridker PM, MacFadyen JG, Thuren T, Everett BM, Libby P, Glynn RJ, et al. Effect of interleukin-1β inhibition with canakinumab on incident lung cancer in patients with atherosclerosis: exploratory results from a randomised, double-blind, placebo-controlled trial. The Lancet 2017;390(10105):1833–42 doi 10.1016/S0140-6736(17)32247-X.

37. Mantovani A, Allavena P, Sica A, Balkwill F. Cancer-related inflammation. Nature 2008;454(7203):436–44 doi 10.1038/nature07205. [PubMed: 18650914]

38. Wang L, Ma Q, Yao R, Liu J. Current status and development of anti-PD-1/PD-L1 immunotherapy for lung cancer. International Immunopharmacology 2020;79:106088 doi 10.1016/j.intimp.2019.106088. [PubMed: 31896512]

39. Reyes-Caballero H, Park B, Loube J, Sanchez I, Vinayachandran V, Choi Y, et al. Immune modulation by chronic exposure to waterpipe smoke and immediate-early gene regulation in murine lungs. Tobacco Control 2020;29(Suppl 2):s80 doi 10.1136/tobaccocontrol-2019-054965. [PubMed: 31852817]

40. Jiang Y, Wang X, Hu D. Mitochondrial alterations during oxidative stress in chronic obstructive pulmonary disease. Int J Chron Obstruct Pulmon Dis 2017;12:1153–62 doi 10.2147/copd.S130168. [PubMed: 28458526]

41. Kantrowitz J, Sinjab A, Xu L, McDowell TL, Sivakumar S, Lang W, et al. Genome-Wide Gene Expression Changes in the Normal-Appearing Airway during the Evolution of Smoking-

Author Manuscript Author Manuscript Author Manuscript Author Manuscript

Associated Lung Adenocarcinoma. Cancer prevention research (Philadelphia, Pa) 2018;11(4):237–48 doi 10.1158/1940-6207.Capr-17-0295.

42. Kadara H, Scheet P, Wistuba II, Spira AE. Early Events in the Molecular Pathogenesis of Lung Cancer. Cancer prevention research (Philadelphia, Pa) 2016;9(7):518–27 doi 10.1158/1940-6207.capr-15-0400.
43. Zang R, Gomez Castro MF, McCune BT, Zeng Q, Rothlauf PW, Sonnek NM, et al. TMPRSS2 and TMPRSS4 promote SARS-CoV-2 infection of human small intestinal enterocytes. Sci Immunol 2020;5(47) doi 10.1126/sciimmunol.abc3582.
44. Cai G, Bossé Y, Xiao F, Kheradmand F, Amos CI. Tobacco Smoking Increases the Lung Gene Expression of ACE2, the Receptor of SARS-CoV-2. American journal of respiratory and critical care medicine 2020;201(12):1557–9 doi 10.1164/rccm.202003-0693LE. [PubMed: 32329629]
45. Bodas M, Moore AR, Subramaniyan B, Georgescu C, Wren JD, Freeman WM, et al. Cigarette Smoke Activates NOTCH3 to Promote Goblet Cell Differentiation in Human Airway Epithelial Cells. American journal of respiratory cell and molecular biology 2021;64(4):426–40 doi 10.1165/rcmb.2020-0302OC. [PubMed: 33444514]
46. Polverino F Cigarette Smoking and COVID-19: A Complex Interaction. American journal of respiratory and critical care medicine 2020;202(3):471–2 doi 10.1164/rccm.202005-1646LE. [PubMed: 32530714]
47. Bahelah R, DiFranza JR, Ward KD, Eissenberg T, Fouad FM, Taleb ZB, et al. Waterpipe smoking patterns and symptoms of nicotine dependence: The Waterpipe Dependence in Lebanese Youth Study. Addict Behav 2017;74:127–33 doi 10.1016/j.addbeh.2017.06.003. [PubMed: 28624697]
48. Malaeb D, Akel M, Sacre H, Haddad C, Obeid S, Hallit S, et al. Association between cumulative cigarette and Waterpipe smoking and symptoms of dependence in Lebanese adults. BMC public health 2021;21(1):1583- doi 10.1186/s12889-021-11626-7. [PubMed: 34425819]
49. Hallit S, Zoghbi M, Hallit R, Youssef L, Costantine R, Kheir N, et al. Effect of exclusive cigarette smoking and in combination with waterpipe smoking on lipoproteins. J Epidemiol Glob Health 2017;7(4):269–75 doi 10.1016/j.jegh.2017.08.006. [PubMed: 29110868]
50. Jawad M, El Kadi L, Mugharbil S, Nakkash R. Waterpipe tobacco smoking legislation and policy enactment: a global analysis. Tobacco Control 2015;24(Suppl 1):i60 doi 10.1136/tobaccocontrol-2014-051911. [PubMed: 25550418]

Author Manuscript Author Manuscript Author Manuscript Author Manuscript

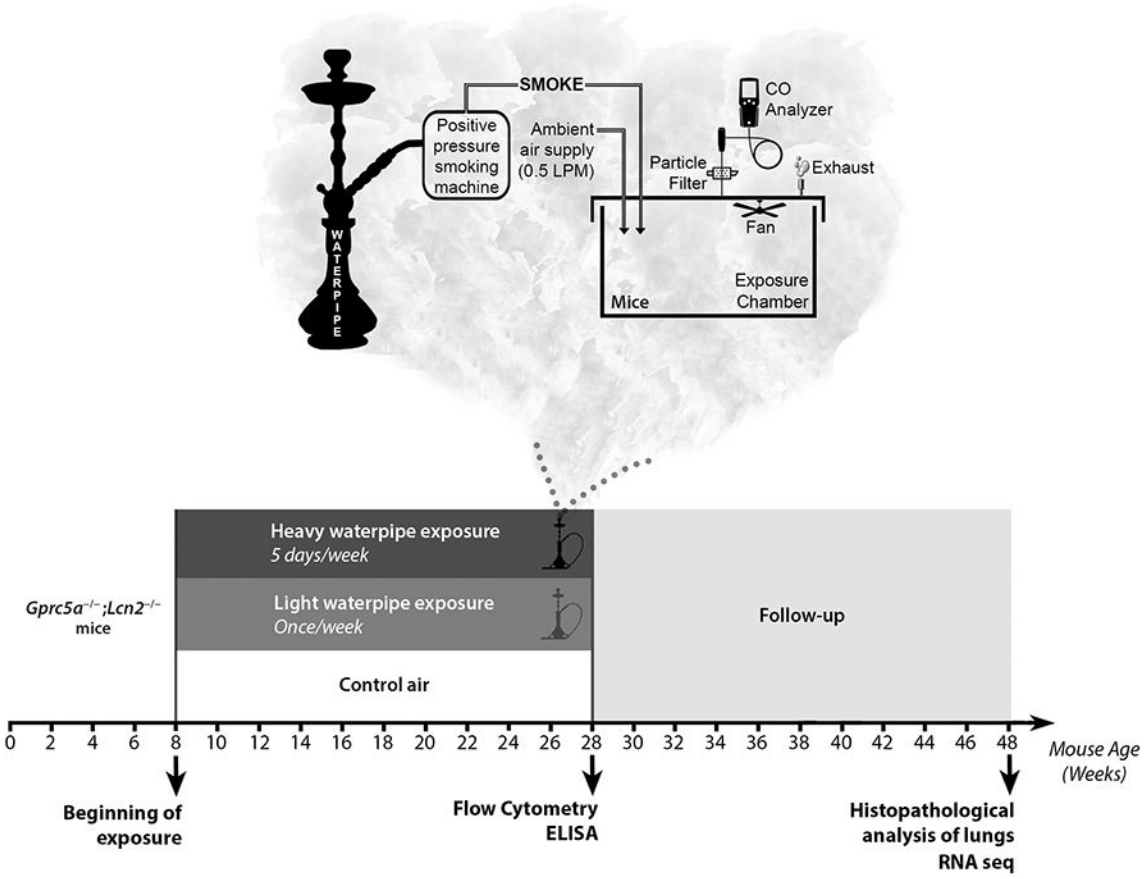

Figure 1. Experimental design and waterpipe exposure apparatus.

Schematic design depicting the whole body waterpipe smoke exposure system. Smoke is drawn intermittently by a positive pressure smoking machine and discharged into a transparent polycarbonate chamber (38x25x25 cm) containing the animals. During the exposure event, ambient air is continuously piped into the chamber at a flow rate of 0.5 LPM. A CO analyzer (Bacharach Monoxor III) is used to monitor the CO levels in the chamber, and a fan is suspended to ensure uniform aerosol concentrations throughout the chamber. A glass fiber filter (Gelman Type A/E) is placed upstream of the CO monitor to allow gravimetric determination of the mean total particulate matter concentration during each exposure session. For the control group, the smoking machine remains off during each exposure session, and animals are exposed to ambient air only. **Lower panel.** Schematic timeline depicting the three experimental exposure groups composed of eight weeks-old *Gprc5a*$^{-/-}$;*Lcn2*$^{-/-}$ mice divided into groups of up to five mice (per exposure group) and studied at the end of exposure, and 20 weeks after completion of exposure. Mice were exposed to WPS for once a week (light WPS) or five times a week (heavy WPS).

Author Manuscript Author Manuscript Author Manuscript Author Manuscript

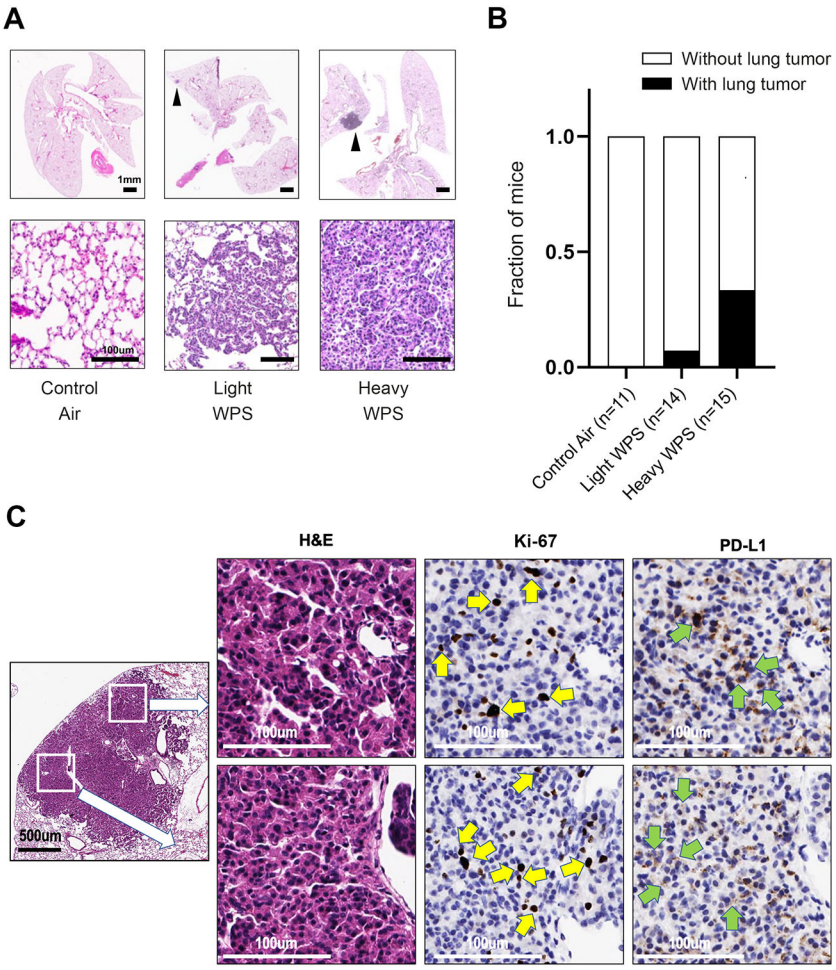

Figure 2. Effects of chronic waterpipe exposure on lungs of mice.

A. Representative histopathologic (H&E) images of lungs from control air, light WPS, and heavy WPS-exposed mice with lesions indicated by black arrows. The scale bars denote 1 mm (upper panel) and 100 μm (lower panel). **B.** Fraction of mice developing lung lesions following control air, light WPS, and heavy WPS exposure. **C.** Representative photomicrographs of positive Ki-67 staining in tumor lung tissues of mice exposed to WPS (indicated by yellow arrows) and PD-L1 staining on epithelial cells in tumors (indicated by green arrows).

Author Manuscript Author Manuscript Author Manuscript Author Manuscript

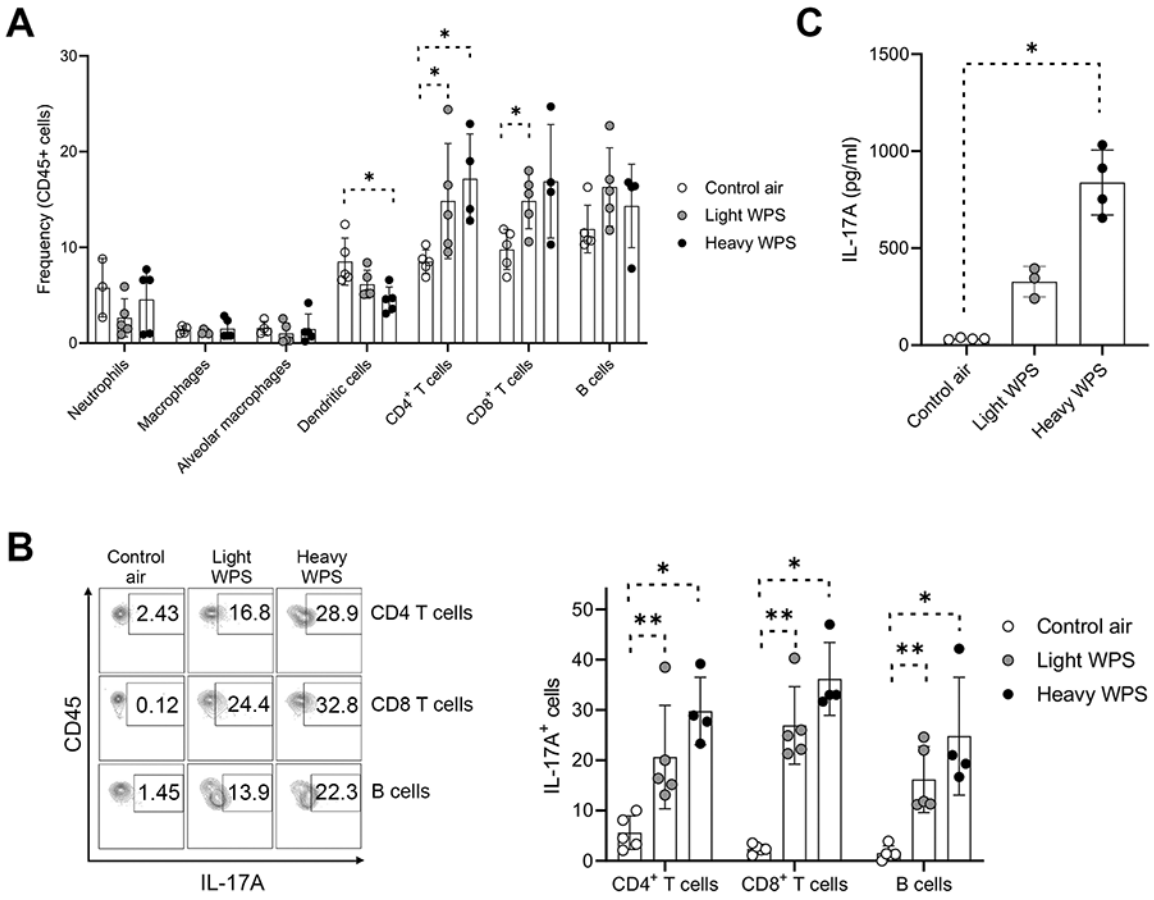

Figure 3. Exposure to WPS induces an inflammatory response in lungs of mice.

A. Flow cytometry analysis of the frequencies of various immune cells after 20 weeks of exposure to control air, light WPS, and heavy WPS in lungs of *Gprc5a*$^{-/-}$;*Lcn2*$^{-/-}$ mice. **B.** Flow cytometry analysis of IL-17A expression in CD4+ T cells, CD8+ T cells and B cells after 20 weeks of exposure to control air, light WPS, and heavy WPS in lungs of *Gprc5a*$^{-/-}$;*Lcn2*$^{-/-}$ mice. **C.** IL-17A ELISA of BALF obtained from *Gprc5a*$^{-/-}$;*Lcn2*$^{-/-}$ cells after 20 weeks of exposure to control air, light WPS, and heavy WPS. Differences between two groups were statistically examined using the Student's *t*-test. *, $P < 0.05$; **, $P < 0.01$; ***, $P < 0.001$.

Author Manuscript Author Manuscript Author Manuscript Author Manuscript

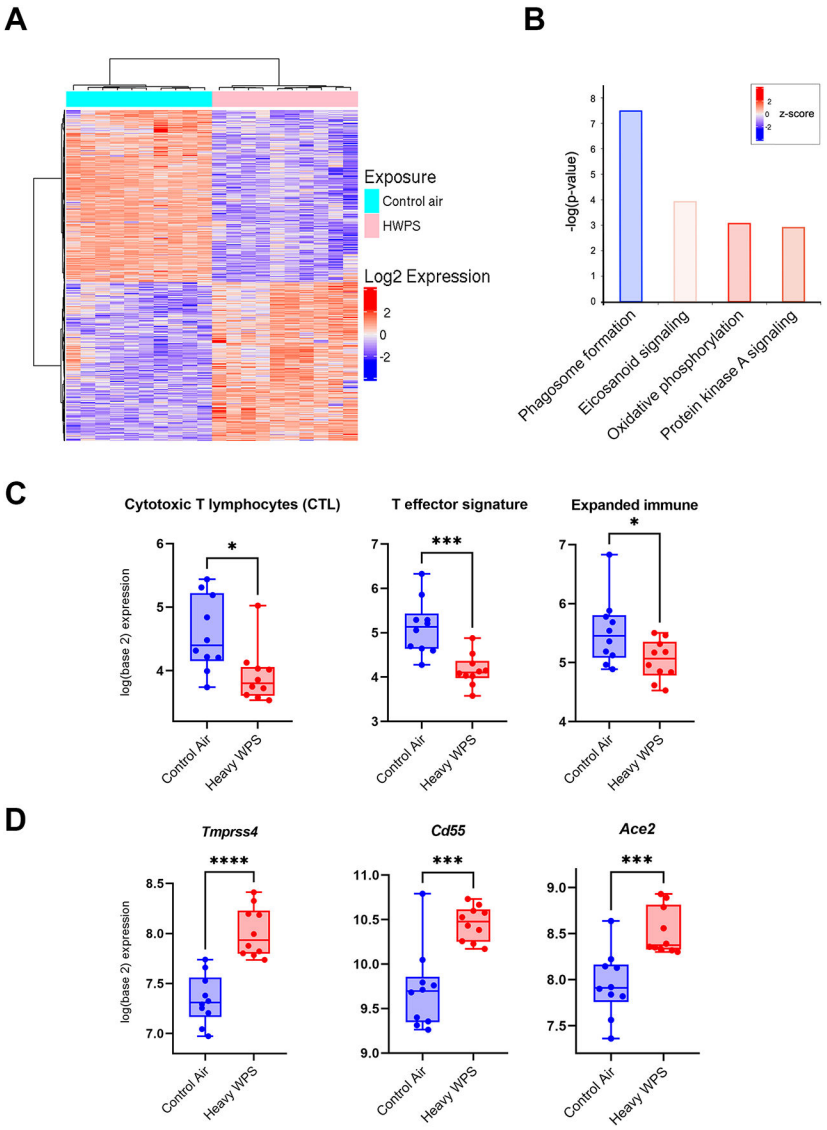

Figure 4. Waterpipe exposure suppresses key anti-tumor immune functions and elevates expression of receptors for the novel coronavirus SARS-CoV-2.

A. Heat map showing differentially expressed transcripts between lungs exposed to control air or heavy WPS and identified by RNA-seq. Columns indicate samples and rows denote transcripts (red, relatively up-regulated; blue, down-regulated). **B.** Enriched pathways in heavy WPS-exposed lung tissues were identified using Ingenuity Pathways Analysis (IPA). Activation of the pathway is indicated by z-scores (red, up-regulated; blue, down-regulated). **C.** The following immune cell signatures indicative of different phenotypes were propagated and computed for each sample as described in Methods: cytotoxic T lymphocyte (CTL), expanded immune, and T effector signature. Immune cell signatures were then statistically compared between control air- (blue) and heavy WPS-exposed (red) lung tissues using the Wilcoxon rank sum test. **D.** *Tmprss4*, *Cd55*, and *Ace2* mRNA expression levels were statistically compared between control air- (blue) and heavy WPS-exposed (red) mice using the Student's *t*-test. *, $P < 0.05$; **, $P < 0.01$; ***, $P < 0.001$.

Author Manuscript Author Manuscript Author Manuscript Author Manuscript

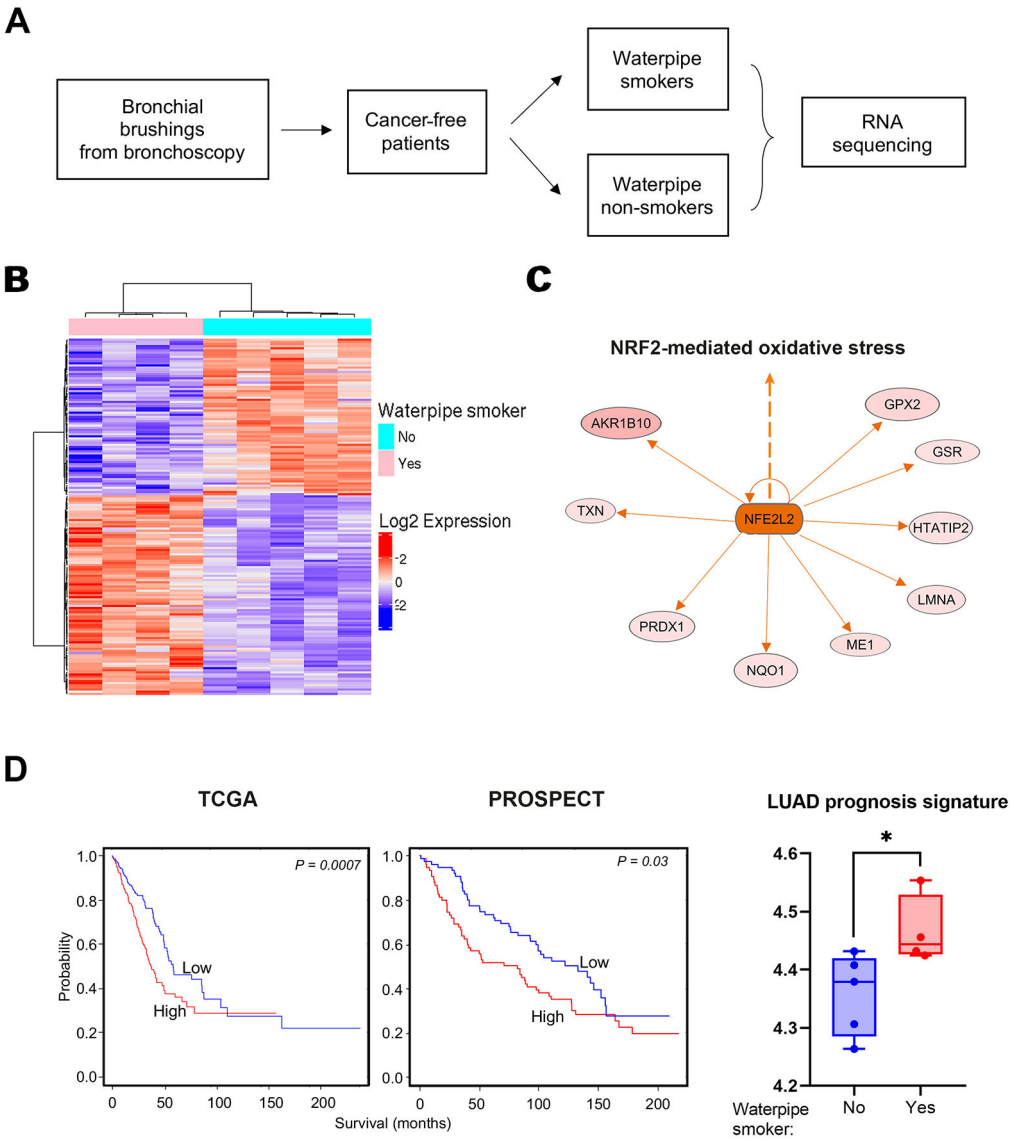

Figure 5. Gene signatures related to lung cancer aggressiveness in airways of human waterpipe smokers.

A. Schematic depicting human cohort selection for RNA seq of bronchial brushings among those undergoing bronchoscopy. **B.** Heat map showing differentially expressed transcripts between human airways of waterpipe smokers compared to non-smokers. Columns indicate patient airways and rows indicate transcripts (red, relatively up-regulated; blue, down-regulated). **C.** Topological network analysis of genes associated with NRF2-mediated oxidative stress in human** airways of waterpipe smokers were derived using IPA. Predicated activation of NRF2-mediated oxidative stress based on the gene set is indicated by the orange color. **D. Left:** Kaplan–Meier of overall survival of patients from TCGA and PROSPECT cohorts stratified by median expression of the WPS-associated prognosis signature (red: relatively higher than the median; blue: lower than the median). **Right:** Lung adenocarcinoma prognosis signature was propagated and computed as described in Methods. The prognosis signature was then statistically compared between non-smokers (blue) and

Author Manuscript Author Manuscript Author Manuscript Author Manuscript

waterpipe smokers (red) using the Wilcoxon rank sum test. *, $P < 0.05$; **, $P < 0.01$; ***, $P < 0.001$.